EUROPEAN RESPIRATORY *journal*

FLAGSHIP SCIENTIFIC JOURNAL OF ERS

Early View

Original article

Transcriptomic investigation reveals donor specific gene signatures in human lung transplants

Cristina Baciu, Andrew Sage, Ricardo Zamel, Jason Shin, Xiao-Hui Bai, Olivia Hough, Mamatha Bhat, Jonathan C Yeung, Marcelo Cypel, Shaf Keshavjee, Mingyao Liu

Please cite this article as: Baciu C, Sage A, Zamel R, *et al*. Transcriptomic investigation reveals donor specific gene signatures in human lung transplants. *Eur Respir J* 2020; in press (https://doi.org/10.1183/13993003.00327-2020).

This manuscript has recently been accepted for publication in the *European Respiratory Journal*. It is published here in its accepted form prior to copyediting and typesetting by our production team. After these production processes are complete and the authors have approved the resulting proofs, the article will move to the latest issue of the ERJ online.

Transcriptomic investigation reveals donor specific gene signatures in human lung transplants

Cristina Baciu[1], Andrew Sage[1], Ricardo Zamel[1], Jason Shin[1], Xiao-Hui Bai[1], Olivia Hough[1], Mamatha Bhat[2,3], Jonathan C Yeung[1,2,4], Marcelo Cypel[1,2,4,5], Shaf Keshavjee*[1,2,4,5], Mingyao Liu*[1,2,4,5]

Affiliations:

[1]Latner Thoracic Surgery Research Laboratories, Toronto General Hospital Research Institute, University Health Network

[2]Multiorgan Transplant Program, University Health Network

[3]Division of Gastroenterology, University of Toronto

[4]Toronto Lung Transplant Program, Department of Surgery, University of Toronto

[5]Institute of Medical Science, University of Toronto

*These authors share senior authorship.

Corresponding author:

Mingyao Liu, MD (mingyao.liu@utoronto.ca)

Professor of Surgery and Director of Institute of Medical Science,

Faculty of Medicine, University of Toronto

James and Mary Davie Chair in Lung Injury, Repair and Regeneration

Latner Thoracic Surgery Research Laboratories, University Health Network

101 College Street, PMCRT2-814, Toronto, Ontario, M5G 1L7 Canada

Phone: (416)-634-7501

Take home message: Lungs from DBD donors have increased activation of inflammatory pathways. In contrast, cell death, apoptosis and necrosis are activated in lungs from DCD donors. EVLP and non-EVLP lungs have also distinct transcriptomic signatures.

Main text word count: 3,135

Abstract

Rationale: Transplantation of lungs from donation after circulatory death (DCD) in addition to donation after brain death (DBD) became routine worldwide to address the global organ shortage. The development of ex vivo lung perfusion (EVLP) for donor lung assessment and repair contributed to the increased use of DCD lungs. We hypothesize that better understanding of the differences between lungs from DBD and DCD donors, and between EVLP and directly transplanted (non-EVLP) lungs, will lead to discovery of the injury specific targets for donor lung repair and reconditioning.

Methods: Tissue biopsies from human DBD (n=177) and DCD (n=65) donor lungs assessed with or without EVLP, were collected at the end of cold ischemic time. All samples were processed with microarray assay. Gene expression, network and pathway analyses were performed using R, Ingenuity Pathway Analysis and STRING. Results were validated with protein assay, multiple logistic regression and 10-fold cross validation.

Results: Our analyses showed that lungs from DBD donors have up-regulation of inflammatory cytokines and pathways. In contrast, DCD lungs display a transcriptome signature of pathways associated with cell death, apoptosis and necrosis. Network centrality revealed specific drug targets to rehabilitate the DBD lungs. Moreover, in DBD lungs, TNFR1/2 signalling pathways and macrophage migration inhibitory factor associated pathways were activated in the EVLP group. A panel of genes that differentiate the EVLP from non-EVLP group in DBD lungs was identified.

Conclusion: The examination of gene expression profiling indicates that DBD and DCD lungs have distinguishable biological transcriptome signatures.

Abstract word count: 246

Keywords: lung transplantation, donation after brain death, donation after circulatory death, inflammation, cell death, ex vivo lung perfusion.

Introduction

Lung transplantation is a life-saving therapy for patients with end-stage lung disease. However, there is a significant shortage of donor lungs to meet this therapeutic need. When compared to other organs, the utilization rate of donated lungs is the lowest, which further exacerbates the organ shortage and leads to an increased mortality rate for patients on the transplant wait list [1]. This is partially caused by the lower availability of lungs from conventional donation after brain death (DBD), compared with other organs [2], as lungs are more vulnerable during retrieval and preservation.

Utilization of lungs from donation after circulatory death (DCD), in addition to DBD lungs has become world-wide practice to increase the number of donor organs for transplantation [3, 4]. According to the International Society for Heart and Lung Transplantation Registry report, the percentage of lung transplants from DCD donors was 20.9% in 2017, and the post-transplant survival for recipients receiving lungs from DCD versus DBD donors is comparable [5, 6].

The development of the ex-vivo lung perfusion (EVLP) technology has increased the utilization of donor lungs, as it enables further organ assessment, treatment, and rehabilitation of donor lungs at body temperature [7, 8]. By providing the donor lung with perfusion and ventilation in a normothermic environment, EVLP can help restore physiological metabolism so that more accurate assessments and more effective therapies are possible prior to transplantation. The use of EVLP for extended criteria donor lungs has led to a 20% increase in available donor lungs for transplant as of 2015 [9], and this number has surged even further over the past four years. Lungs assessed by EVLP that progress to transplant have similar post-transplant outcomes compared with standard donor lungs [10, 11]. Better understanding of the differences between DCD and

DBD lungs, and identification of the indications for proceeding to EVLP will be crucial to finding precise therapeutic targets and deciding which lungs would benefit from EVLP.

The present study aims to answer the following two questions: (i) are DBD and DCD donor lungs different at the transcriptional level, and (ii) do EVLP and non-EVLP lungs have different gene signature at cold ischemic time?

There is a lack of systematic investigation of transcriptional signatures specific to donor types. A pilot study using microarray data from 12 DBD and 6 DCD human lung samples, performed by our group [12], showed more inflammation-related genes in DBD lungs compared to lungs from DCD donors. However, the sample size at the time was very small, lacking in statistical power, details on the inflammatory genes and pathways were very limited, and a comparison of EVLP vs. non-EVLP samples was not performed. The objective of the current study was to examine a large data set of human lungs to conduct comprehensive bioinformatics and systems biology analyses to answer the questions above, and to validate the findings of our previous work, giving that the validation using a different cohort of samples is extremely important.

Materials and Methods

Donor lungs, RNA Extraction and Microarrays

The donor peripheral lung tissue biopsies were collected at the end of cold ischemic time (CIT) before EVLP or transplant, and snap frozen in liquid nitrogen by the Toronto Lung Transplant Program, at University Health Network, from 2010 to 2015. Total RNA was extracted, then purified using RNeasy Mini Kit (Qiagen; Hilden, Germany). RNA quality was verified by Nanodrop spectrophotometer (VWR; Radnor, PA) and Bioanalyzer (Agilent; Santa Clara, CA).

All samples were processed with Clariom D™ Assay (Thermo Fisher Scientific; Waltham, MA). Raw data and processed files are accessible at GEO, series accession number GSE128204 (Reviewer Access Token: "sdspwogkzvuhzah").

General clinical indications to select donor lungs for EVLP were defined by following criteria: ratio of the partial pressure of arterial oxygen to the fraction of inspired oxygen (PO_2:FiO_2) less than 300 mm Hg, presence of pulmonary edema or infiltrates on chest imaging.

This study was approved by the University Health Network research ethics boards (REB#11-0509 and REB#12-5488) and ethics review board of the Trillium Gift of Life Network. All patients provided written consent for tissue bio-banking.

Bioinformatics analyses

The entire flow of bioinformatics analyses and the corresponding methods is depicted in Supplementary Figure 1.

Gene expression and clustering analysis

We have selected only those samples that were transplanted directly or following EVLP. The lungs rejected for transplant were not considered.

There are several group comparisons defined in this study (Table 1). (I) all DBD (n=177) vs. all DCD (n=65); (II) non-EVLP DBD (n=123) vs. non-EVLP DCD (n=22); (III) EVLP DBD (n=54) vs. EVLP DCD (n=43); (IV) EVLP DCD (n=43) vs. non-EVLP DCD (n=22); and (V) EVLP DBD (n=54) vs. non-EVLP DBD (n=123) lung samples.

Differential gene expression, principal component analysis and hierarchical clustering were performed in R [13] version 3.5.0 with various packages: affy [14], limma [15] annotate [16], pca3d [17]. For heatmap visualization, we employed MetaboAnalyst [18] software. Microarray data was pre-processed by RMA utilizing the affy [14] package. We used the entrez gene ID alternative annotation package from Brainarray [19]. P-values for differential gene expression were obtained using limma [15] package. Batch effects were minimized by adjusting for microarray lot within the limma models. A gene was considered differentially expressed (DE) between two groups if a p-value corrected for False Discovery Rate (FDR) using the Benjamini-Hochberg [20] method, was less than 0.05 (FDR < 0.05). In addition, stronger effects were defined for DE genes with fold change: FC ≥ 2 (up-regulation) or FC ≤ 0.5 (down-regulation), or otherwise indicated.

Pathway and network analysis

The lists of the DE genes and their statistical and experimental parameters (FDR-corrected p-value, $\log_2$FC) corresponding to each group comparison in this study were uploaded to the Ingenuity Systems® (www.ingenuity.com) to perform ingenuity pathway analyses (IPA). For network analysis we employed STRING Database version 10.5 [21] and igraph package [22].

Multiple Logistic Regression and 10-fold cross validation

We investigated the correlation between the seven highly DE genes in EVLP DBD vs. non-EVLP DBD comparison using stepwise multiple logistic regression method. We validated the best model with 10-fold cross validation method. Area under the Curve (AUC) was calculated with ROCR [23] package.

More details on bioinformatics methods are included in the Supplementary Material.

Protein Assays

EVLP perfusate samples of the donor lungs were collected at 1 hour into perfusion. Samples were taken directly from the pulmonary venous outflow and tested on an automated ELISA for IL-6, IL-8 and IL-1β as per manufacturer's instructions (Protein Simple, San Jose, CA).

Results

Clinical data of donors are provided in Table 2. The donors were similar in terms of age, sex, smoking status, chest x-ray infiltration and mechanism of injury leading to brain death (head trauma or anoxia/cardiac arrest) or the decision to withdraw life sustaining therapies in the case of DCDs. The donors with cerebrovascular/stroke were 58.8% in DBD group, compared to 41.5% in DCD group (p-value=0.02). The ratio of last arterial partial pressure of oxygen (PaO_2) to fraction of inspired oxygen (FiO_2), (PaO_2:FiO_2), was significantly higher in DCD group (p-value=0.019), with proportionally more DCD cases being assessed by EVLP (66.15%) as per institutional practice.

Transcriptional signatures show significant differences between DBD and DCD donor lungs

Differential gene expression analysis at FDR ≤ 0.05 revealed 5,196 DE genes in all DBD vs. all DCD comparison, 1,972 DE genes in non-EVLP DBD vs. non-EVLP DCD, and 2,792 DE genes in EVLP DBD vs. EVLP DCD group comparison. These genes displayed a fair separation between DBD and DCD groups by Principal Component Analysis (Supplementary Figure 2 a-c). Genes with fold change FC ≥ 2 or FC ≤ 0.5 (Supplementary Table 1) showed a very good delineation between DBD and DCD samples, as presented by heat maps with unsupervised

hierarchical clustering (Figure 1). The large numbers of DE genes and the distinct gene clustering between DBD and DCD lungs indicate that the pathophysiological conditions of these two types of organ donations are quite different.

Inflammation is dominant in DBD lungs and cell death is associated with DCD lungs

Within the list of highly DE genes in DBD vs. DCD samples identified based on FDR and fold change (FC $\geq$ 2 or FC $\leq$ 0.5), 18 are common to all 3 group comparisons and are highly up-regulated (Supplementary Table 1). Among them are: (i) members of the chemokine family (*CCL2, CXCL2, CXCL8 (i.e., IL-8)*) involved in immunoregulatory and inflammatory processes [24]; (ii) genes from Nuclear Receptor Subfamily 4 (*NR4A1, NR4A2, NR4A3*), shown to regulate neutrophil lifespan and homeostasis [25]; (iii) several metallothioneins (*MT1M, MT1G, MT1X, MT1A, MT1JP*) involved in cellular homeostasis, but also in differentiation and proliferation of normal and tumour cells, tumor angiogenesis [26], and (iv) others, e.g. *AMADTS4* and *SELE* with established roles in fibrosis [27], and *FOSB* - a regulator of cell proliferation, differentiation, and transformation [28].

There are nine DE genes shared between EVLP and All samples, of which chemokine *CCL20* and cytokine *IL-6* are well known for their role in inflammatory responses. There are several DE genes exclusive to the EVLP group. Of these, activation of *IL-1β* and *PTX3* have been linked to donor lung injury or poor outcome after lung transplantation [29, 30]. The up-regulated *NFKBIZ* gene in EVLP lung group, which encodes the transcription factor IκBζ, is associated with increased susceptibility to invasive pneumococcal disease [31]. *IER3*, found to be activated in EVLP category of lungs, has roles in immune responses, inflammation, and tumorigenesis and rheumatoid arthritis [32].

Following the gene expression analysis, we investigated the pathways, diseases and functions associated with DE genes using IPA. In comparison with DCD lungs, the majority of canonical pathways are up-regulated and very few are down-regulated in DBD samples (Table 3). Among the up-regulated pathways common to all three comparisons, IL-6 Signaling, HMGB1 Signaling, TREM1 Signaling, and p38 MAPK Signaling are known to play roles in pulmonary inflammation, infections and immune responses. Of the pathways, specific to EVLP samples were: IL-1 Signaling, LPS-stimulated MAPK Signaling, NRF2-mediated Oxidative Stress Response, Role of IL-17F in Allergic Inflammatory Airway Diseases and iNOS Signaling are activated in DBD donor lungs. These are pathways prominent in inflammation [7, 33-35]. The detailed information on p-value and z-score of these pathways are given in Supplementary Table 2.

IPA predicted a wide range of activated diseases and functions in DBD vs. DCD samples. More specifically, cell viability and cell survival pathways frequently seen in tumor-related research are activated in DBD, while cell death, apoptosis and necrosis related pathways are activated in DCD samples (Figure 2).

Network centrality reveals specific drug targets to potentially rehabilitate DBD lungs

For network analysis, we performed a STRING analysis using the three short lists of highly DE genes (Supplementary Table 1), without protein-protein interactors from the database. The resulting networks have protein-protein interaction enrichment p-values < 1.0E-16 (Figure 3), suggesting that these are very strong biological networks solely based on DE genes between DBD and DCD lung samples.

The central node is IL-6 for biological networks derived from either all DBD vs. DCD lungs (Figure 3a; betweenness score = 29.3) or using EVLP only samples (Figure 3c; betweenness

score = 41.8). These results also reflect the pathway analysis that lists IL-6 as the top altered pathway (Table 3). For non-EVLP samples only (Figure 3b), the central node was NR4A1 (betweenness score = 18.5). The centrality analysis could be important for drug targeting. For instance, targeting IL-6 may result in the inhibition of the entire network, thus triggering inhibition of inflammation. More mechanistic and experimental studies are necessary to test this hypothesis.

EVLP lungs are different from non-EVLP lungs at the transcriptomic level

Comparisons of the EVLP DBD (n=54) and non-EVLP DBD (n=123) samples revealed 401 DE genes. Pathway analysis showed the involvement of genes in TNF family member receptors, TNFR1/2 signaling pathways, and in macrophage migration inhibitory factor (MIF) - related pathways in the EVLP lungs (Supplementary Figure 3), which supports inflammatory responses as potential therapeutic targets for DBD lung repair during EVLP [36]. These pathways are known to exert potent pro-inflammatory effects and regulate immune responses [35, 37, 38]. Several genes are shared by these pathways, including *NFKB1* (NFκB subunit 1), *NFKBIE* (NFκB inhibitor epsilon), *NFKBIA* (NFκB inhibitor alpha), *BIRC3* (also called Inhibitor of Apoptosis Protein 1), and *PLA2G5* (Phospholipase A2 Group V, a secretory enzyme that can induce inflammatory responses in neighbouring cells) (Supplementary Table 3), indicating these pathways are highly related to each other.

Further filtering the DE genes by FDR < 0.05 and FC ≥ 1.5 or FC ≤ 0.7 identified eight genes (*SCGB1A1, C20orf85, CFAP126, SNTN, FAM216B, MS4A8, TSPAN1, LOC101928817*) down-regulated in EVLP samples (Figure 4a). From this list we excluded the non-characterized gene (*LOC101928817*) with unknown function. To validate these results, we performed multiple

logistic regression analysis, which showed high correlation among the other seven DE genes (Figure 4b). This implies that each of these genes could be predictive of EVLP assessment on its own. The step procedure determined that the best model was with *CFAP126* (Cilia and Flagella Associated Protein 126)*;* the 10-fold cross validation showed 70% prediction accuracy, with an area under the curve value (AUC) = 0.70, (Figure 4c).

Comparison of non-EVLP DCD lungs (n=22) vs. EVLP DCD lungs (n=43) resulted in no significant differences at the transcriptional level. This may be due to the small number of DCD donor lungs in our dataset, and to the fact that EVLP has been more frequently used for DCD lungs at our center (66% in Table 2).

Experimental validation

In an effort to recapitulate our findings at the transcript level, we performed parallel protein work using perfusate samples collected during EVLP after the first hour. Consistent with our transcript data, there was a significantly higher concentration of IL-6, IL-8 and IL-1β proteins from DBD donors in comparison with DCD donors (Figure 5).

Discussion

Our study demonstrated that the lung injuries in DBD and DCD lungs arise from different biological mechanisms, as evidenced by their different respective transcriptomic signatures. With this work, we have validated the results from our previous pilot study showing that lungs from DBD donors present higher inflammation [12], and we further revealed details on activation of immunological diseases and immune responses. IL-6, HMGB1, TREM1, and p38MAPK signaling pathways were found to be activated in DBD vs. DCD comparisons. In addition, as a novelty of our study, we also found that the activation of cell death, apoptosis and necrosis

pathways were associated with DCD donor lungs. We further identified IL-6 as a central node for a network of highly DE genes in DBD lungs, especially in lungs assessed with EVLP. These results will be very valuable for further drug targeting studies, since it demonstrates that the two types of donor lungs may require different types of treatment.

To our knowledge, this is the first large-scale study of human lungs, aiming to identify the transcriptional differences, molecular pathways and networks between DBD and DCD donor lungs used for transplantation. The results at the transcript level between DBD and DCD lungs were also partially confirmed at the protein level, in perfusate samples taken at one hour after the start of EVLP. This confirms that the pathway activation reported here does lead to translational changes at the protein level in the lung, as demonstrated by the protein assays on the common molecules (IL-6, IL-8, IL-1β) present in IL-6, HMGB1 and TREM1 signaling pathways.

EVLP provides the means to evaluate extended criteria donor lungs, thus increasing the number of utilized lungs for transplantation, and reducing the risk of using poor quality donor lungs. EVLP also provides the opportunity to repair or to improve donor lung quality. Identification of possible drug targets for different types of lung injuries is critical, and our study revealed genes and pathways that mediates inflammation and/or cell death as potential targets for lung repair during EVLP. Recently, we have shown alpha-1 antitrypsin reduced porcine donor lung injury by inhibiting acute inflammatory responses and cell death during EVLP [39]. It is possible to use this or other anti-inflammatory and/or anti-cell death drugs to repair human donor lungs during EVLP. Hozain and colleagues have developed xenogeneic cross-circulation for extracorporeal recovery of injured human lungs [40], which provides a new platform for donor lung repair.

In current transplantation practice, clinical experience dictates which extended lungs are directed to EVLP. Our analyses revealed molecular differences between EVLP and non-EVLP samples.

First, the heat maps of DE genes of the DBD vs. DCD lungs comparisons look more similar between all samples and EVLP-only samples, than with non-EVLP lungs (Figure 1). Second, significant pathways from all sample comparison shows more overlap with EVLP-only samples than with non-EVLP samples (Table 3). Thirdly, the biological networks derived from highly DE genes from all or from EVLP-only samples shared the same central node, IL-6 (Figure 3).

We have further shown that activation of inflammatory pathways is characteristic of lungs selected for EVLP, as TNFR1/2 signalling pathways and MIF-mediated pathways are activated in the EVLP group. A group of genes highly differentiate the EVLP group from the non-EVLP group in DBD samples. This panel of DE genes could be further tested and developed, to facilitate clinical decision making on which DBD donor lungs should be subjected to EVLP assessment, and repair. One of the limitations of this study is the smaller number of non-EVLP vs. EVLP samples in the DCD lungs group, as DCD was a relatively new practice during 2011-2015 when the samples were collected. Due to the uncertainty of using DCD lungs, the majority of DCD lungs have been proceeded to EVLP in our program. The differences between non-EVLP and EVLP group in DCD group are currently unknown. The second limitation is the relatively small number of EVLP perfusate samples tested for IL-6, IL-8 and IL-1β by protein assays. These cases were part of a prospective validation study for cytokine biomarkers to assess the donor lung repair. As such we used all samples so far collected. We also recognize the importance of investigating the outcome from lung transplant, e.g. using gene expression as biomarkers to predicate donor lungs that may develop primary graft dysfunction after transplantation, which constitutes the objective of a future investigation and cannot be addressed in the present study.

Overall, our findings constitute important information for the clinical lung transplantation community, delineating different types of donor specific lung injuries, and providing important clues to potential actionable drug targets to facilitate donor lung recovery for subsequent transplantation. The EVLP signature reflects that based on current criteria on which EVLP was assigned, these lungs have distinct transcriptomic features that are different from those of directly transplanted lungs. These results provide deeper understanding on donor lung biology, and although the immediate clinical implication of these findings remains unclear, it is hoped that they will ultimately help us to improve donor lung management, increase the number of lungs available for transplantation and potentially even improve lung allograft outcomes.

Author Contributions

CB participated in the study design, performed all bioinformatics analyses, submitted the raw data to GEO and wrote the manuscript; AS performed protein analysis; RZ provided raw microarray data and revised the manuscript; JS and XB performed experimental validation; OH prepared the figures; MB, MC, JCY assisted with review and editing; SK led the bio-banking and microarray studies; ML and SK conceived the study design and supervised the project; all authors revised the final draft of the manuscript.

Funding: Canadian Institutes of Health Research (operating grants MOP-31227, MOP-119514 and PJT-148847) and Genome Canada (Genomic Application Partnership Program grant #6427).

Declaration of Interest: Authors declare no conflicts of interests.

References:

1. Jawoniyi O, Gormley K, McGleenan E, Noble HR. Organ donation and transplantation: Awareness and roles of healthcare professionals—A systematic literature review. *J Clin Nurs* 2018: 27(5-6): e726-e738.

2. and Klein AS, Messersmith EE, Ratner LE, Kochik R, Baliga PK, Ojo AO. Organ donation utilization in the United States, 1999-2008. *Am J Transplant* 2010: 10(4 Pt 2): 973-986.

3. Munshi L, Keshavjee S, Cypel M. Donor management and lung preservation for lung transplantation. *Lancet Resp Med* 2013: 1(4): 318-328.

4. Cypel M, Levvey B, Van Raemdonck D, Erasmus M, Dark J, Love R, Mason D, Glanville AR, Chambers D, Edwards LB, Stehlik J, Hertz M, Whitson BA, Yusen RD, Puri V, Hopkins P, Snell G, Keshavjee S. International Society for Heart and Lung Transplantation Donation After Circulatory Death Registry Report. *J Heart Lung Transplant* 2015: 34(10): 1278-1282.

5. Krutsinger D, Reed RM, Blevins A, Puri V, De Oliveira NC, Zych B, Bolukbas S, Raemdonck DV, Snell GI, Eberlein M. Lung transplantation from donation after cardiocirculatory death: a systematic review and meta-analysis. *J Heart Lung Transplant* 2015: 34(5): 675-684.

6. Villavicencio MA, Axtell AL, Spencer PJ, Heng EE, Kilmarx S, Dalpozzal N, Funamoto M, Roy N, Osho A, Melnitchouk S, D'Alessandro DA, Tolis G, Astor T. Lung Transplantation From Donation After Circulatory Death: United States and Single-Center Experience. *Ann Thorac Surgery* 2018.

7. Cypel M, Yeung JC, Liu M, Anraku M, Chen F, Karolak W, Sato M, Laratta J, Azad S, Madonik M, Chow C-W, Chaparro C, Hutcheon M, Singer LG, Slutsky AS, Yasufuku K, de Perrot M, Pierre AF, Waddell TK, Keshavjee S. Normothermic Ex Vivo Lung Perfusion in Clinical Lung Transplantation. *N Engl J Med* 2011: 364(15): 1431-1440.

8. Cypel M. Ex vivo lung perfusion (EVLP). *Curr Respir Care Rep* 2013: 2: 167–172.

9. Reeb JK, Shaf; Cypel, Marcelo. Expanding the lung donor pool: advancements and emerging pathways. *Curr Opin Organ Transplant* 2015: 20(5): 498–505.

10. Cypel M, Yeung JC, Machuca T, Chen M, Singer LG, Yasufuku K, de Perrot M, Pierre A, Waddell TK, Keshavjee S. Experience with the first 50 ex vivo lung perfusions in clinical transplantation. *J Thorac Cardiovasc Surg* 2012: 144(5): 1200-1206.
11. Tikkanen JM, Cypel M, Machuca TN, Azad S, Binnie M, Chow C-W, Chaparro C, Hutcheon M, Yasufuku K, de Perrot M, Pierre AF, Waddell TK, Keshavjee S, Singer LG. Functional outcomes and quality of life after normothermic ex vivo lung perfusion lung transplantation. *J Heart Lung Transplant* 2015: 34(4): 547-556.

12. Kang CH, Anraku M, Cypel M, Sato M, Yeung J, Gharib SA, Pierre AF, de Perrot M, Waddell TK, Liu M, Keshavjee S. Transcriptional signatures in donor lungs from donation after cardiac death vs after brain death: A functional pathway analysis. *J Heart Lung Transplant* 2011: 30(3): 289-298.

13. R Core Team. R: A language and environment for statistical computing. *R Foundation for Statistical Computing,Vienna, Austria* 2013.

14. Gautier L, Cope L, Bolstad BM, Irizarry RA. affy—analysis of Affymetrix GeneChip data at the probe level. *Bioinformatics* 2004: 20(3): 307-315.

15. Ritchie ME, Phipson B, Wu D, Hu Y, Law CW, Shi W, Smyth GK. limma powers differential expression analyses for RNA-sequencing and microarray studies. *Nucleic Acids Res* 2015: 43(7): e47-e47.

16. Gentleman R. annotate: Annotation for microarrays. 2018.

17. January W. pca3d: Three Dimensional PCA Plots. 2017.

18. Chong J, Soufan O, Li C, Caraus I, Li S, Bourque G, Wishart DS, Xia J. MetaboAnalyst 4.0: towards more transparent and integrative metabolomics analysis. *Nucleic Acids Res* 2018: 46(W1): W486-W494.

19. MacDonald JW. clariomdhumantranscriptcluster.db: Affymetrix clariomdhuman annotation data (chip clariomdhumantranscriptcluster). 2017.

20. Benjamini Y, Hochberg Y. Controlling the False Discovery Rate: A Practical and Powerful Approach to Multiple Testing. *J Royal Stat Soc Series B Methodol* 1995: 57(1): 289-300.

21. Szklarczyk D, Franceschini A, Wyder S, Forslund K, Heller D, Huerta-Cepas J, Simonovic M, Roth A, Santos A, Tsafou KP, Kuhn M, Bork P, Jensen LJ, von Mering C.

STRING v10: protein–protein interaction networks, integrated over the tree of life. *Nucleic Acids Res* 2015: 43(D1): D447-D452.

22. Gabor C, Tamas N. The igraph software package for complex network research. *IJ Comp Sys* 2006: Complex Systems(5): 1695.

23. Beerenwinkel N, Sander O, Lengauer T, Sing T. ROCR: visualizing classifier performance in R. *Bioinformatics* 2005: 21(20): 3940-3941.

24. Turner MD, Nedjai B, Hurst T, Pennington DJ. Cytokines and chemokines: At the crossroads of cell signalling and inflammatory disease. *Biochim Biophys Acta Mol Cell Res* 2014: 1843(11): 2563-2582.

25. Prince LR, Prosseda SD, Higgins K, Carlring J, Prestwich EC, Ogryzko NV, Rahman A, Basran A, Falciani F, Taylor P, Renshaw SA, Whyte MKB, Sabroe I. NR4A orphan nuclear receptor family members, NR4A2 and NR4A3, regulate neutrophil number and survival. *Blood* 2017: 130(8): 1014.

26. Si M, Lang J. The roles of metallothioneins in carcinogenesis. *J Hematol Oncol* 2018: 11(1): 107.

27. Steele MP, Luna LG, Coldren CD, Murphy E, Hennessy CE, Heinz D, Evans CM, Groshong S, Cool C, Cosgrove GP, Brown KK, Fingerlin TE, Schwarz MI, Schwartz DA, Yang IV. Relationship between gene expression and lung function in Idiopathic Interstitial Pneumonias. *BMC Genomics* 2015: 16(1): 869.

28. Milde-Langosch K. The Fos family of transcription factors and their role in tumourigenesis. *Eur J Cancer* 2005: 41(16): 2449-2461.

29. Cypel M, Kaneda H, Yeung JC, Anraku M, Yasufuku K, de Perrot M, Pierre A, Waddell TK, Liu M, Keshavjee S. Increased levels of interleukin-1β and tumor necrosis factor-α in donor lungs rejected for transplantation. *J Heart Lung Transplant* 2011: 30(4): 452-459.

30. Yoshida M, Oishi H, Martinu T, Hwang DM, Takizawa H, Sugihara J, McKee TD, Bai X, Guana Z, Lua C, Cho H-R, Juvet S, Cypel M, Keshavjee S, Liu M. Pentraxin 3 Deficiency Enhances Features of Chronic Rejection in a Mouse Orthotopic Lung Transplantation Model. *Oncotarget* 2018: 9(9): 8489-8501.

31. Sundaram K, Rahman MA, Mitra S, Knoell DL, Woodiga SA, King SJ, Wewers MD. IκBζ Regulates Human Monocyte Pro-Inflammatory Responses Induced by Streptococcus pneumoniae. *PLoS One* 2016: 11(9): e0161931-e0161931.

32. Morinobu A, Tanaka S, Nishimura K, Takahashi S, Kageyama G, Miura Y, Kurosaka M, Saegusa J, Kumagai S. Expression and Functions of Immediate Early Response Gene X-1 (IEX-1) in Rheumatoid Arthritis Synovial Fibroblasts. *PLoS One* 2016: 11(10): e0164350-e0164350.

33. Liu M. Nitric oxide synthase gene expression in lung transplantation. *Acta Pharmacol Sinica* 1997: 18(6): 548-550.

34. Liu M, Tremblay L, Cassivi SD, Bai X-H, Mourgeon E, Pierre AF, Slutsky AS, Post M, Keshavjee S. Alterations of nitric oxide synthase expression and activity during rat lung transplantation. *Am J Physiol-Lung Cell Mol Physiol* 2000: 278(5): L1071-L1081.

35. Sakiyama S, Hamilton J, Han B, Jiao Y, Shen-Tu G, de Perrot M, Keshavjee S, Liu M. Activation of Mitogen-activated Protein Kinases During Human Lung Transplantation. *J Heart Lung Transplant* 2005: 24(12): 2079-2085.

36. Wang A, Zamel R, Yeung J, Bader G, Dos Santos C, Bai X, Wang Y, Keshavjee S, Liu M. Potential Therapeutic Targets for Lung Repair During Human Ex Vivo Lung Perfusion *Eur Respir J* 2020: 55(4): 1902222.

37. Ting AT, Bertrand MJM. More to Life than NF-κB in TNFR1 Signaling. *Trends Immunol* 2016: 37(8): 535-545.

38. Subbannayya T, Variar P, Advani J, Nair B, Shankar S, Gowda H, Saussez S, Chatterjee A, Prasad TSK. An integrated signal transduction network of macrophage migration inhibitory factor. *J Cell Commun Signal* 2016: 10(2): 165-170.

39. Lin H, Chen M, Tian F, Tikkanen J, Ding L, Andrew Cheung HY, Nakajima D, Wang Z, Mariscal A, Hwang D, Cypel M, Keshavjee S, Liu M. α1-Anti-trypsin improves function of porcine donor lungs during ex-vivo lung perfusion. *J Heart Lung Transplant* 2018: 37(5): 656-666.

40. Hozain AE, O'Neill JD, Pinezich MR, Tipograf Y, Donocoff R, Cunningham KM, Tumen A, Fung K, Ukita R, Simpson MT, Reimer JA, Ruiz EC, Queen D, Stokes JW, Cardwell NL, Talackine J, Kim J, Snoeck HW, Chen YW, Romanov A, Marboe CC, Griesemer AD, Guenthart BA, Bacchetta M, Vunjak-Novakovic G. Xenogeneic cross-

circulation for extracorporeal recovery of injured human lungs. *Nat Med* 2020: 26(7): 1102-1113.

Figure legend

Figure 1. Differentially expressed genes between DBD and DCD lungs. Heat maps with differentially expressed genes by strict filtering (FDR≤0.05, FC≥2 or FC≤0.5) with unsupervised hierarchical clustering: **a)** all samples, DBD vs. DCD; **b)** Non-EVLP samples, DBD vs. DCD; **c)** EVLP samples, DBD vs. DCD. FC, fold change; DBD, donation after brain death; DCD, donation after circulatory death; EVLP, ex-vivo lung perfusion.

Figure 2. Ingenuity Pathway Analysis shows different diseases and functions for all samples, DBD vs. DCD comparison. DBD, donation after brain death; DCD, donation after circulatory death.

Figure 3. Highly differentially expressed genes are functionally connected as networks. STRING networks with differentially expressed genes by strict filtering (FDR < 0.05; FC≥2 or FC≤0.5): **a**) all samples, DBD vs. DCD; **b)** Non-EVLP samples, DBD vs. DCD; **c)** EVLP samples, DBD vs. DCD. The black arrows with the corresponding text indicate the central nodes. Only connected nodes are shown. FDR, False Discovery Rate; FC, fold change; DBD, donation after brain death; DCD, donation after circulatory death; EVLP, ex-vivo lung perfusion.

Figure 4. Differentially expressed genes in DBD lungs (EVLP vs. non-EVLP). **a**) Volcano plot showing highly differentially expressed (DE) genes (blue dots) by filtering criteria: FDR < 0.05 and FC ≥ 1.5 or FC ≤ 0.7, in DBD samples (EVLP vs. non-EVLP); **b**) Logistic regression model shows high correlation between the seven differentially expressed genes for DBD (EVLP vs. non-EVLP) lungs at the end of CIT. The numbers represent the correlation coefficients and the red stars denote statistical significance, p-value<0.001; **c**) ROC curve for the best model (CFAP126) determined by stepwise procedure. CIT, cold ischemic time pre-transplant or pre-

EVLP. DBD, donation after brain death; FDR, False Discovery Rate; FC, fold change; EVLP, ex-vivo lung perfusion.

Figure 5. Selected cytokines levels (aligned dot plots with median and interquartile range) in: **a)** lung tissue – microarray data; **b)** EVLP perfusate – protein level. DBD, donation after brain death; DCD, donation after circulatory death; EVLP, ex-vivo lung perfusion. Statistical analyses were performed with 2-tailed non-parametric Mann-Whitney test.

Table 1. Human lung samples used in this study.

Sample type	DBD	DCD
Non-EVLP	123	22
EVLP	54	43
Total	**177**	**65**

DBD, donation after brain death;

DCD, donation after circulatory death;

EVLP, ex-vivo lung perfusion.

Table 2. DBD and DCD donor characteristics.

Characteristic	**DBD** (n=177)	**DCD** (n=65)	**p-value**
Age (years)	45.65 (17.60)	45.97 (17.57)	0.902
Sex			0.772
M	87 (49.15%)	34 (52.31%)	
F	90 (50.85%)	31 (47.69%)	
Donor smoking	89 (42.94%)	37 (61.66%)	0.545
Mechanism leading to brain death or irreversible brain injury			
Cerebrovascular/Stroke	104 (58.76%)	27 (41.54%)	0.020
Head trauma	37 (20.90%)	19 (29.23%)	0.173
Anoxia/Cardiac arrest	27 (15.25%)	16 (24.61%)	0.128
Donor last PaO_2/FIO_2	386.9 (105.0)	421.87 (86.9)	0.019
Chest X-ray infiltration	80 (45.20%)	35 (53.85%)	0.429
EVLP	54 (30.51%)	43 (66.15%)	7.69e-07

Data are n (%) or mean standard deviation (SD). Statistical p-value is calculated

with Fisher's exact test, except for numerical data (age, donor last PaO_2/FIO_2) where t-test was applied. PaO_2, partial pressure of arterial oxygen; FIO_2, fraction of inspired oxygen; DBD, donation after brain death; DCD, donation after circulatory death.

Table 3. Summary of the pathways activated or inhibited in DBD vs. DCD sample

Pathway	All samples	Non-EVLP	EVLP
IL-6 Signaling	y	y	y
HMGB1 Signaling	y	y	y
TREM1 Signaling	y	y	y
p38 MAPK Signaling	y	y	y
ERK5 Signaling	y	y	y
MIF-mediated Glucocorticoid Regulation	y	y	
Acute Phase Response Signaling	y		y
Hypoxia Signaling in the Cardiovascular System	y		y
LXR/RXR Activation	y		y
Pyridoxal 5'-phosphate Salvage Pathway	y		y
B Cell Receptor Signaling	y		
Complement System	y		
MIF Regulation of Innate Immunity	y		

Th1 Pathway	y	
iCOS-iCOSL Signaling in T Helper Cells	y	
1D-myo-inositol Hexakisphosphate Biosynthesis II		y
AMPK Signaling		y
Chondroitin Sulfate Biosynthesis		y
Dermatan Sulfate Biosynthesis		y
ERK/MAPK Signaling		y
Valine Degradation I		y
IL-1 Signaling		y
LPS-stimulated MAPK Signaling		y
NRF2-mediated Oxidative Stress Response		y
Role of IL-17F in Allergic Inflammatory Airway Diseases		y
iNOS Signaling		y
IL-17A Signaling in Gastric Cells		y
4-1BB Signaling in T Lymphocytes		y
Aryl Hydrocarbon Receptor Signaling		y
Lymphotoxin β Receptor Signaling		y
PI3K Signaling in B Lymphocytes		y
Salvage Pathways of Pyrimidine Ribonucleotides		y

In grey are shown the inhibited pathways in DBD lung (or activated in DCD).

Everything else is activated in DBD samples. EVLP, ex-vivo lung perfusion.

DBD, donors after brain death; DCD, donation after circulatory death.

a. All samples,
DBD vs. DCD

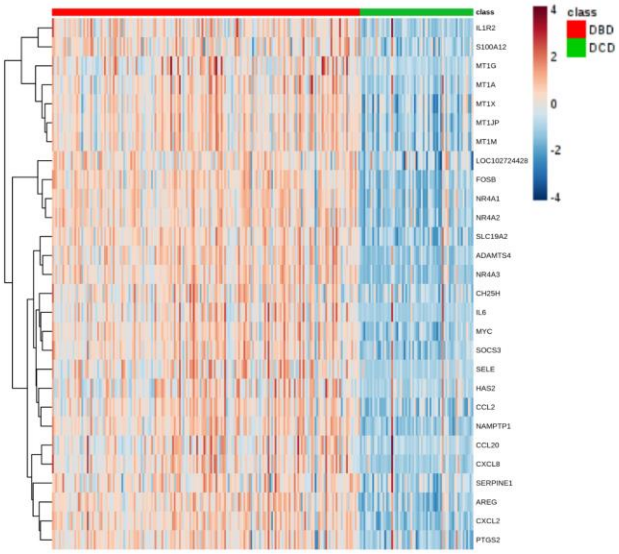

b. Non-EVLP samples,
DBD vs. DCD

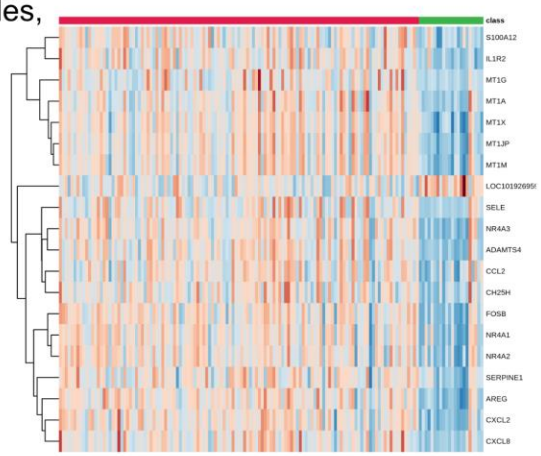

c. EVLP samples,
DBD vs. DCD

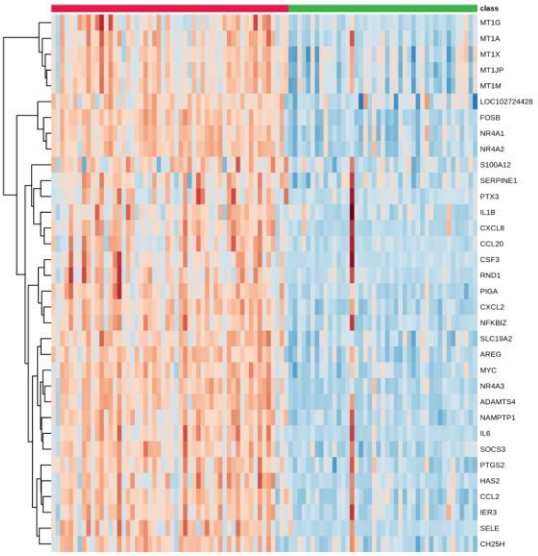

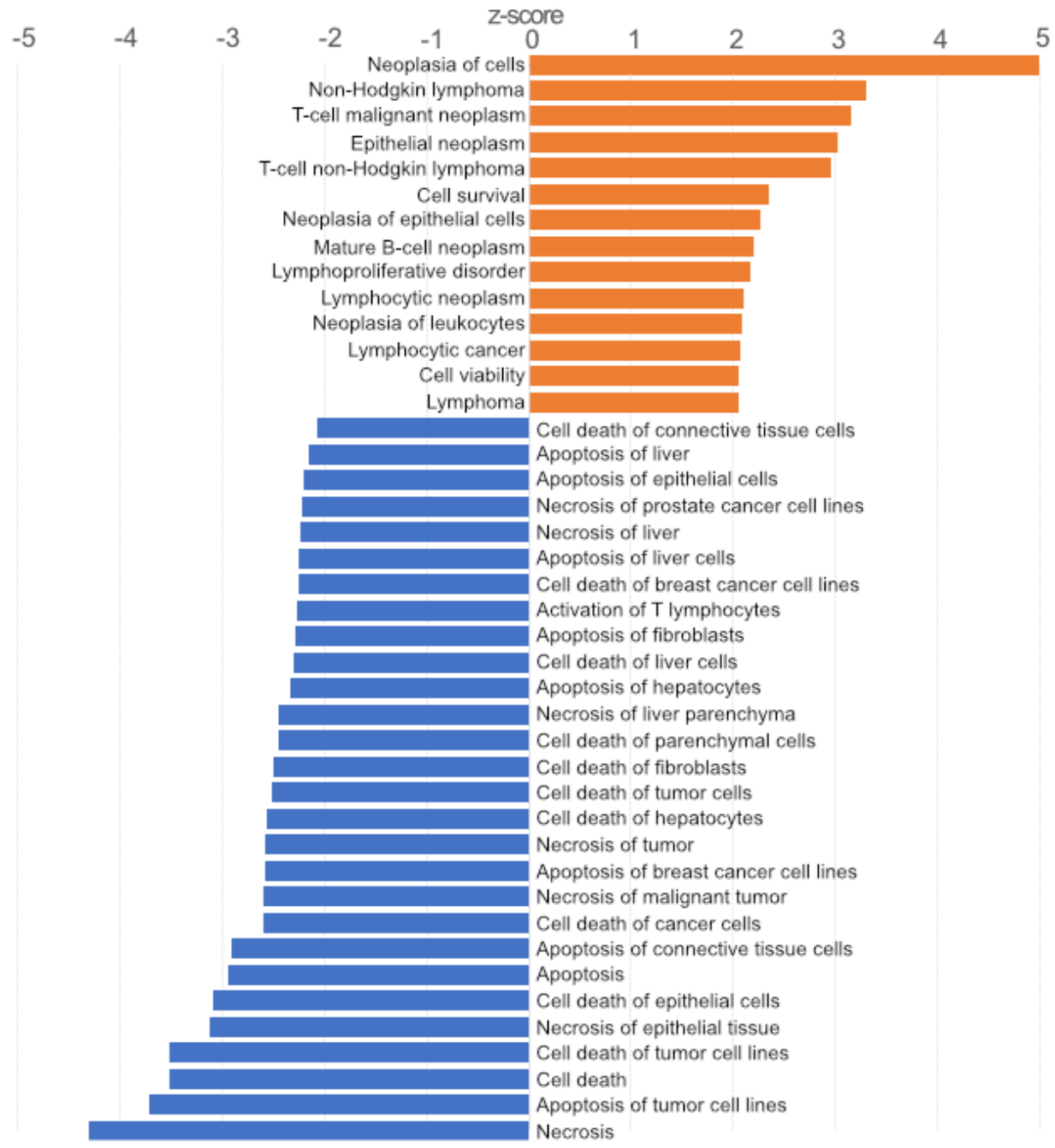
z-score
-5
-4
-3
-2
-1
0
1
2
3
4
5
Neoplasia of cells
Non-Hodgkin lymphoma
T-cell malignant neoplasm
Epithelial neoplasm
T-cell non-Hodgkin lymphoma
Cell survival
Neoplasia of epithelial cells
Mature B-cell neoplasm
Lymphoproliferative disorder
Lymphocytic neoplasm
Neoplasia of leukocytes
Lymphocytic cancer
Cell viability
Lymphoma
Cell death of connective tissue cells
Apoptosis of liver
Apoptosis of epithelial cells
Necrosis of prostate cancer cell lines
Necrosis of liver
Apoptosis of liver cells
Cell death of breast cancer cell lines
Activation of T lymphocytes
Apoptosis of fibroblasts
Cell death of liver cells
Apoptosis of hepatocytes
Necrosis of liver parenchyma
Cell death of parenchymal cells
Cell death of fibroblasts
Cell death of tumor cells
Cell death of hepatocytes
Necrosis of tumor
Apoptosis of breast cancer cell lines
Necrosis of malignant tumor
Cell death of cancer cells
Apoptosis of connective tissue cells
Apoptosis
Cell death of epithelial cells
Necrosis of epithelial tissue
Cell death of tumor cell lines
Cell death
Apoptosis of tumor cell lines
Necrosis

a) All samples, DBD vs. DCD

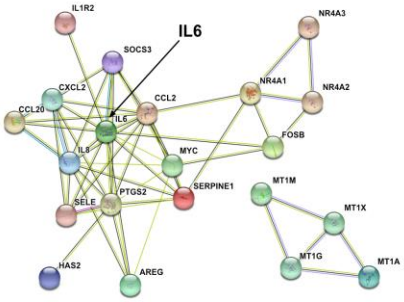

b) Non-EVLP samples, DBD vs. DCD

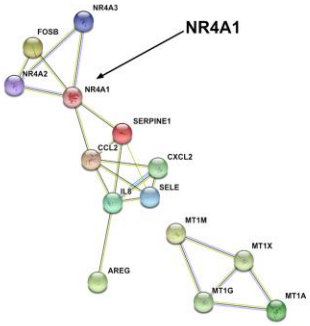

c) EVLP samples, DBD vs. DCD

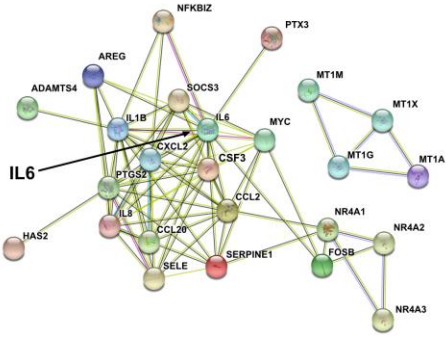

Known Interactions
- from curated databases
- experimentally determined

Predicted Interactions
- gene neighborhood
- gene fusions
- gene co-occurrence

Others
- textmining
- co-expression
- protein homology

Node Color
- colored nodes: query proteins and first shell of interactors
- white nodes: second shell of interactors

a. Volcano plot, EVLP vs. non-EVLP, DBD lungs

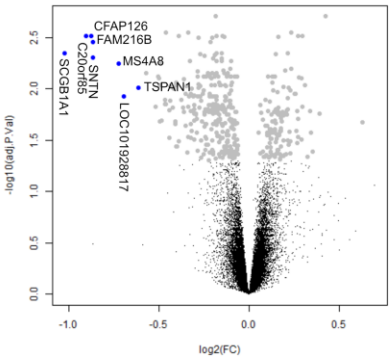

b. Correlation plot

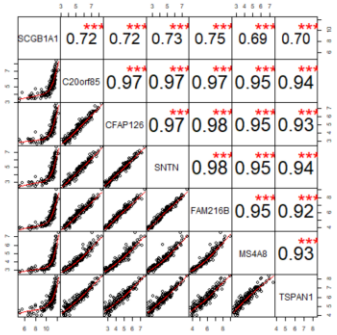

c. ROC curve

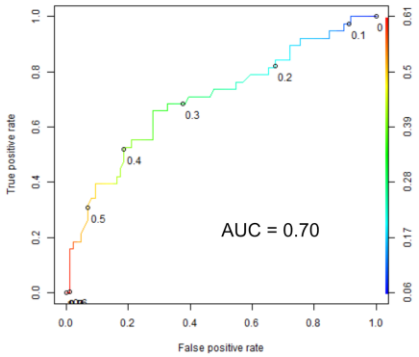

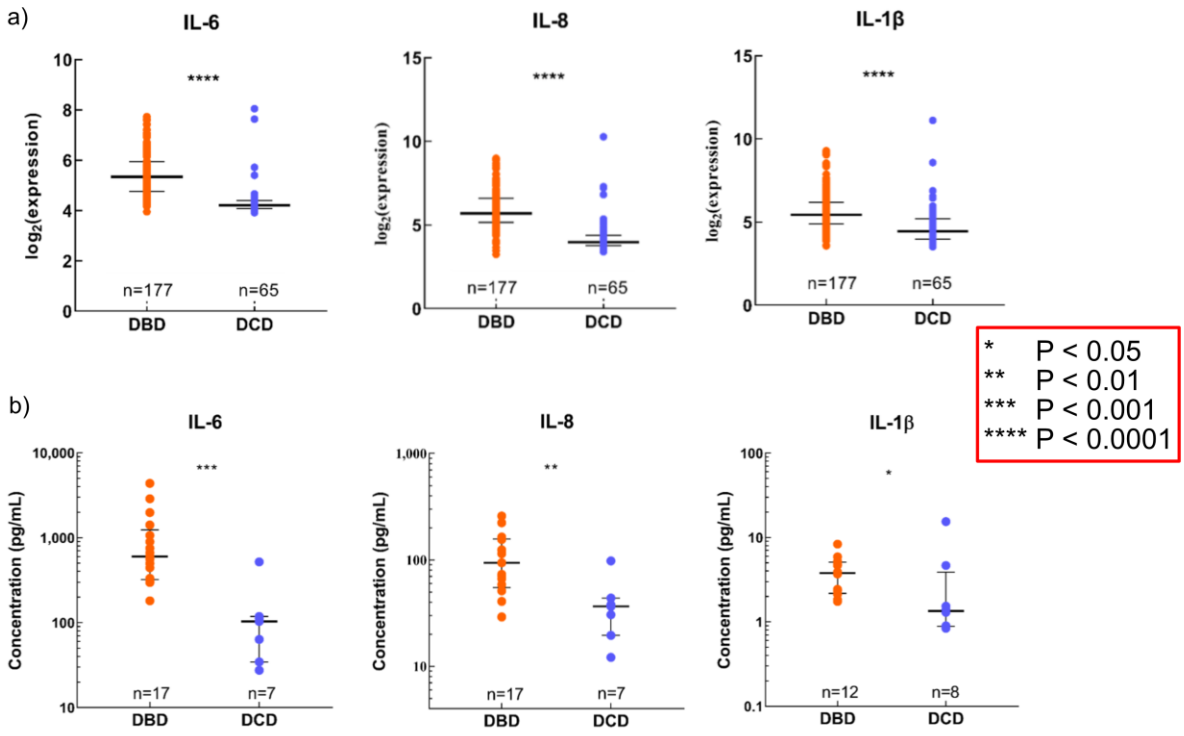
a)
IL-6
IL-8
IL-1β
log2(expression)
****
n=177
n=65
DBD
DCD
b)
Concentration (pg/mL)
***
**
*
n=17
n=7
n=12
n=8
* P < 0.05
** P < 0.01
*** P < 0.001
**** P < 0.0001

Supplementary Material

Transcriptomic investigation reveals donor specific gene signatures in human lung transplants

Cristina Baciu[1], Andrew Sage[1], Ricardo Zamel[1], Jason Shin[1], Xiao-Hui Bai[1], Olivia Hough[1], Mamatha Bhat[2,3], Jonathan C Yeung[1,2,4], Marcelo Cypel[1,2,4,5], Shaf Keshavjee*[1,2,4,5], Mingyao Liu*[1,2,4,5]

Affiliations:

[1]Latner Thoracic Surgery Research Laboratories, Toronto General Hospital Research Institute, University Health Network

[2]Multiorgan Transplant Program, University Health Network

[3]Division of Gastroenterology, University of Toronto

[4]Toronto Lung Transplant Program, Department of Surgery, University of Toronto

[5]Institute of Medical Science, University of Toronto

*These authors share senior authorship.

Table of contents

Content	Page
Supplementary Methods	3-5
Supplementary Table 1: Highly differentially expressed genes by fold change, FC (DBD vs. DCD lungs).	6
Supplementary Table 2: Pathway analysis detailed information.	7-8
Supplementary Table 3: Detailed pathway analysis for EVLP vs non-EVLP samples within DBD lungs.	9
Supplementary Fig 1: Flowchart of bioinformatics analyses	10
Supplementary Fig 2: Principal Component Analysis plots	11
Supplementary Fig 3: Pathway Analysis in comparison EVLP DBD vs Non-EVLP DBD lungs	12

Supplementary Methods

Differential gene expression analysis

We have performed microarray gene expression analysis using limma package [1] in R (Version 3.5.0). For data normalization we employed the Robust Multi-array Average (RMA). After having fit the model with lmFit function (linear model), the differential gene expression was calculated using eBayes function (moderated t-test, p-value, B stats). The differential gene expression was calculated between DBD and DCD samples in the three group categories (All samples, EVLP, non-EVLP), or between EVLP and non-EVLP samples within DBD or DCD lung samples. Differentially expressed genes were defined as having an FDR<0.05 using the Benjamin-Hochberg procedure [2] first, and then by fold change, as per main text.

Pathway and network analysis

The lists of the DE genes and their statistical and experimental parameters (FDR-corrected p-value, $\log_2$FC) corresponding to each group comparison in this study, as explained above, were uploaded to the IPA (Ingenuity Systems®, www.ingenuity.com) to perform pathway and network analyses. IPA uses its own, manually curated "Knowledge Database" which gathers data from experiments already validated and published in peer-reviewed journals. A pathway is predicted to be activated or inhibited based on a calculated z-score using a specific algorithm meant to reduce the chance that random data will generate significant predictions. A z-score ≥ 2 implies high activation, and z-score ≤ -2 defines strong inhibition. Statistical p–values were also calculated for each pathway and network, based on the number of input genes and the total number of molecules

known by the IPA Knowledge Database to be present in that network, using a right-tailed Fisher's exact test [3].

Alternatively, for network analysis we also employed STRING Database version 10.5 [4]. The input to STRING was the short list of DE genes identified for each group comparison, strictly filtered by FDR-corrected p-value and fold change cut-off, FC $\geq$ 2 or FC $\leq$ 0.5. The networks created by our input molecules were used for further centrality calculations.

Network centrality analysis

The central nodes of the networks and the betweenness scores were identified and calculated using igraph package [5] (version 1.01) in R (Version 3.5.0), by computing the shortest paths between all the pairs of nodes in the network. Using the betweenness function, we calculated the centrality score of the nodes (vertices) in the corresponding network. A node with higher betweenness centrality would have more control over the network, because more information will pass through that node.

Multiple Logistic Regression and 10-fold cross validation

We investigated the correlation between the seven highly DE genes in EVLP, DBD vs. non-EVLP, DBD comparison using stepwise multiple logistic regression method with a selection of packages: dplyr [6], PerformanceAnalytics [7] and corrplot [8]. We validated the best model with 10-fold cross validation method, using caret [9] package. Area under the Curve (AUC) was calculated with ROCR [10] package.

References

1. Ritchie ME, Phipson B, Wu D, Hu Y, Law CW, Shi W, Smyth GK. limma powers differential expression analyses for RNA-sequencing and microarray studies. *Nucleic Acids Res* 2015: 43(7): e47-e47.

2. Benjamini Y, Hochberg Y. Controlling the False Discovery Rate: A Practical and Powerful Approach to Multiple Testing. *J Royal Stat Soc Series B Methodol* 1995: 57(1): 289-300.

3. Fisher RA. On the Interpretation of χ2 from Contingency Tables, and the Calculation of P. *J Royal Stat Soc Series B Methodol* 1922: 85(1): 87-94.

4. Szklarczyk D, Franceschini A, Wyder S, Forslund K, Heller D, Huerta-Cepas J, Simonovic M, Roth A, Santos A, Tsafou KP, Kuhn M, Bork P, Jensen LJ, von Mering C. STRING v10: protein–protein interaction networks, integrated over the tree of life. *Nucleic Acids Res* 2015: 43(D1): D447-D452.

5. Gabor C, Tamas N. The igraph software package for complex network research. *IJ Comp Sys* 2006: 1695.

6. Wickham H, François R, Henry L, Müller K. dplyr: A Grammar of Data Manipulation., 2019.

7. Peterson BG, Carl P. PerformanceAnalytics: Econometric Tools for Performance and Risk Analysis. R package version 1.5.2. 2018.

8. Wei T, Simko V. R package "corrplot": Visualization of a Correlation Matrix., 2017.

9. Max Kuhn. Contributions from Jed Wing SW, Andre Williams, Chris Keefer, Allan Engelhardt, Tony, Cooper ZM, Brenton Kenkel, the R Core Team, Michael Benesty, Reynald Lescarbeau, Andrew Ziem,, Luca Scrucca YT, Can Candan and Tyler Hunt. caret: Classification and Regression Training. . 2018.

10. Beerenwinkel N, Sander O, Lengauer T, Sing T. ROCR: visualizing classifier performance in R. *Bioinformatics* 2005: 21(20): 3940-3941.

Supplementary Table 1. Fold change (DBD vs. DCD lungs) of highly differentially expressed genes (FDR corrected p-value≤ 0.05 and fold change FC ≥2 or FC ≤ 0.5).

gene	all samples	non-EVLP samples	EVLP samples
CCL2	3.4	2.3	4.8
CXCL2	2.6	2.3	3.2
CXCL8	2.9	2.3	4.1
NR4A1	2.3	2.0	2.6
NR4A2	3.4	2.7	4.5
NR4A3	3.5	2.7	4.9
MT1M	2.4	2.7	2.4
MT1G	2.3	2.1	2.8
MT1X	2.3	2.6	2.2
MT1A	2.2	2.2	2.4
MT1JP	2.0	2.1	2.1
ADAMTS4	4.2	3.5	5.3
SELE	3.3	2.5	4.8
FOSB	4.8	4.1	6.3
SERPINE1	2.0	2.0	2.1
S100A12	2.8	2.6	2.9
CH25H	2.3	2.1	2.7
AREG	2.2	2.2	2.5
IL1R2	2.0	2.1	
CCL20	2.5		3.8
IL6	2.1		2.6
PTGS2	2.2		2.7
NAMPTP1	2.1		2.5
SOCS3	2.1		2.3
MYC	2.0		2.2
LOC102724428	2.0		2.2
HAS2	2.0		2.8
SLC19A2	2.0		2.0
LOC101926959		0.50	
RND1			2.6
IL1β			2.2
PTX3			2.2
NFKBIZ			2.2
IER3			2.2
PIGA			2.1
CSF3			2.1

EVLP, ex-vivo lung perfusion. DBD, donors after brain death; DCD, donation after cardiac death.

Supplementary Table 2. Pathway analysis detailed information. In orange are shown activated pathways, in blue inhibited pathways. DBD, donation after brain death; DCD, donation after circulatory death; EVLP, ex-vivo lung perfusion.

Group	Ingenuity Canonical Pathway	-log(p-value)	zScore
All	ERK5 Signaling	2.73E+00	3.00
(DBD vs DCD)	IL-6 Signaling	4.37E+00	2.65
	TREM1 Signaling	3.57E+00	2.65
	HMGB1 Signaling	3.62E+00	2.59
	Hypoxia Signaling in the Cardiovascular System	2.46E+00	2.50
	Acute Phase Response Signaling	3.27E+00	2.41
	B Cell Receptor Signaling	3.97E+00	2.21
	MIF-mediated Glucocorticoid Regulation	2.37E+00	2.14
	MIF Regulation of Innate Immunity	1.51E+00	2.14
	Pyridoxal 5'-phosphate Salvage Pathway	1.39E+00	2.06
	p38 MAPK Signaling	2.95E+00	2.06
	LXR/RXR Activation	3.83E+00	-2.54
	Complement System	1.71E+00	-2.53
	Th1 Pathway	3.32E+00	-2.33
	iCOS-iCOSL Signaling in T Helper Cells	3.99E+00	-2.06
Non-EVLP	Chondroitin Sulfate Biosynthesis	1.54E+00	3.00
(DBD vs DCD)	Dermatan Sulfate Biosynthesis	1.45E+00	3.00
	TREM1 Signaling	3.29E+00	2.84
	HMGB1 Signaling	1.42E+00	2.84
	p38 MAPK Signaling	3.09E+00	2.83
	IL-6 Signaling	4.54E+00	2.60
	MIF-mediated Glucocorticoid Regulation	1.31E+00	2.45
	AMPK Signaling	1.82E+00	2.36
	ERK/MAPK Signaling	1.38E+00	2.29
	1D-myo-inositol Hexakisphosphate Biosynthesis II	1.90E+00	2.24
	ERK5 Signaling	1.68E+00	2.11
	Valine Degradation I	1.35E+00	-2.00
EVLP	IL-6 Signaling	4.50E+00	3.77
(DBD vs DCD)	p38 MAPK Signaling	3.78E+00	3.13
	Pyridoxal 5'-phosphate Salvage Pathway	1.69E+00	3.05
	NRF2-mediated Oxidative Stress Response	2.08E+00	2.98
	Role of IL-17F in Allergic Inflammatory Airway D	2.07E+00	2.71
	ERK5 Signaling	2.84E+00	2.67
	HMGB1 Signaling	1.60E+00	2.56
	IL-1 Signaling	2.39E+00	2.52
	LPS-stimulated MAPK Signaling	1.39E+00	2.50
	PI3K Signaling in B Lymphocytes	1.97E+00	2.40
	TREM1 Signaling	3.06E+00	2.36
	Acute Phase Response Signaling	3.91E+00	2.26
	4-1BB Signaling in T Lymphocytes	1.74E+00	2.24
	Salvage Pathways of Pyrimidine Ribonucleotides	1.52E+00	2.18

Hypoxia Signaling in the Cardiovascular System	2.64E+00	2.12
iNOS Signaling	1.31E+00	2.12
Lymphotoxin Œ≤ Receptor Signaling	2.34E+00	2.11
Aryl Hydrocarbon Receptor Signaling	1.53E+00	2.06
IL-17A Signaling in Gastric Cells	1.33E+00	2.00
LXR/RXR Activation	3.34E+00	-3.13

Supplementary Table 3: IPA Pathway analysis results in details, for DBD lungs, EVLP vs non-EVLP. DBD, donation after brain death; EVLP, ex-vivo lung perfusion.

Ingenuity Canonical Pathways	-log(p-value)	zScore	Molecules
TNFR2 Signaling	3.01E+00	1.00	NFKB1,NFKBIE,NFKBIA,BIRC3
TWEAK Signaling	2.76E+00	-1.00	NFKB1,NFKBIE,NFKBIA,BIRC3
MIF-mediated Glucocorticoid Regulation	2.67E+00	1.00	NFKB1,NFKBIE,NFKBIA,PLA2G5
MIF Regulation of Innate Immunity	2.32E+00	1.00	NFKB1,NFKBIE,NFKBIA,PLA2G5
Nicotine Degradation II	2.28E+00	-2.24	CYP4B1,CYP4X1,INMT,FMO2
TNFR1 Signaling	2.19E+00	1.00	NFKB1,NFKBIE,NFKBIA,BIRC3
Induction of Apoptosis by HIV1	1.89E+00	-1.00	NFKB1,NFKBIE,NFKBIA,BIRC3
Protein Kinase A Signaling	1.67E+00	1.63	HIST3H3,NFKB1,PPP1R14A,EYA1,PPP1R3C,PTP4A1,CNGA4,AKAP14, PTPRT,NFKBIE,NFKBIA,MYLK3
Antioxidant Action of Vitamin C	1.56E+00	-1.00	NFKB1,NFKBIE,NFKBIA,PLA2G5

activated pathway
inactivated pathway

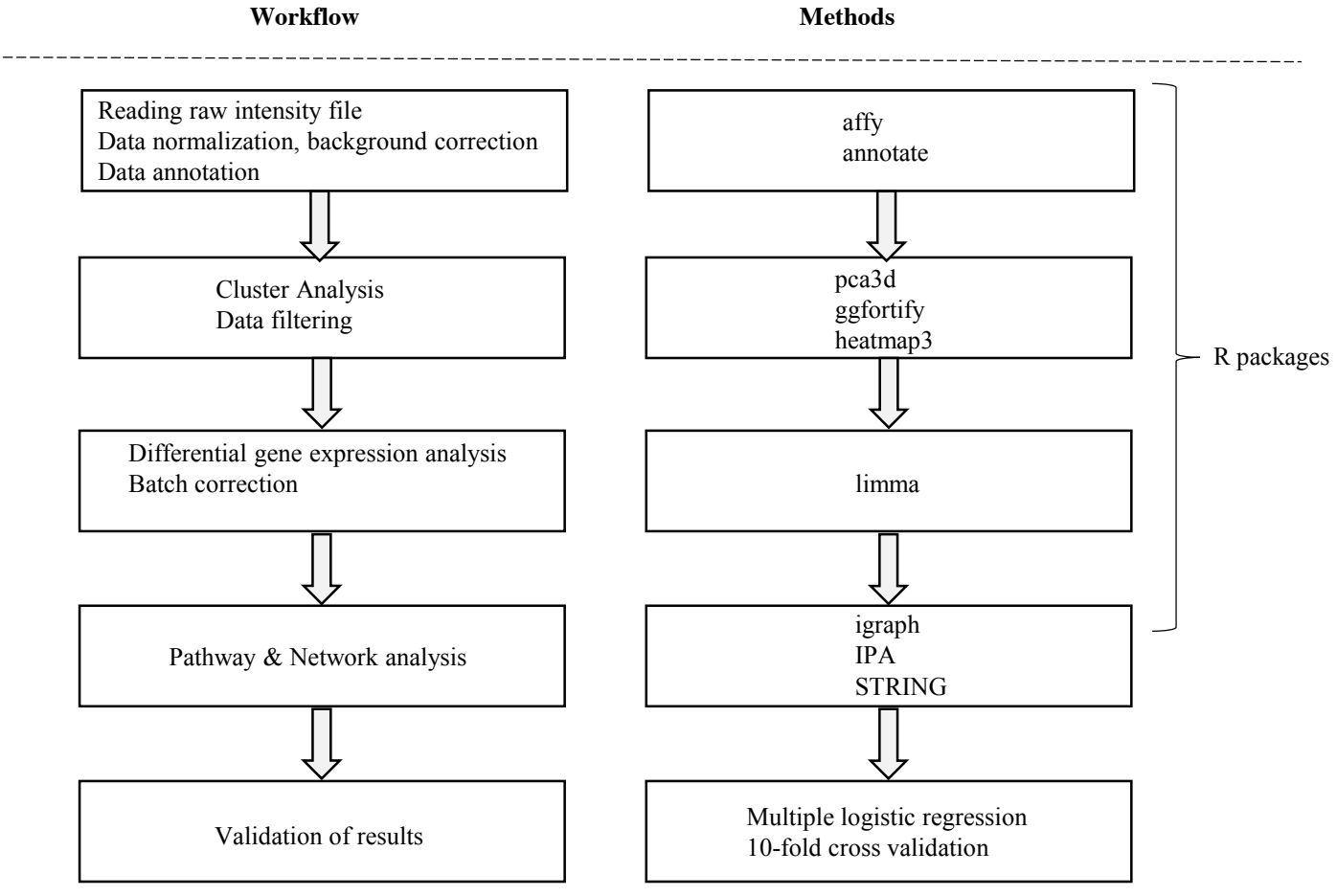

Supplementary Figure 1. Flow chart of bioinformatics analysis

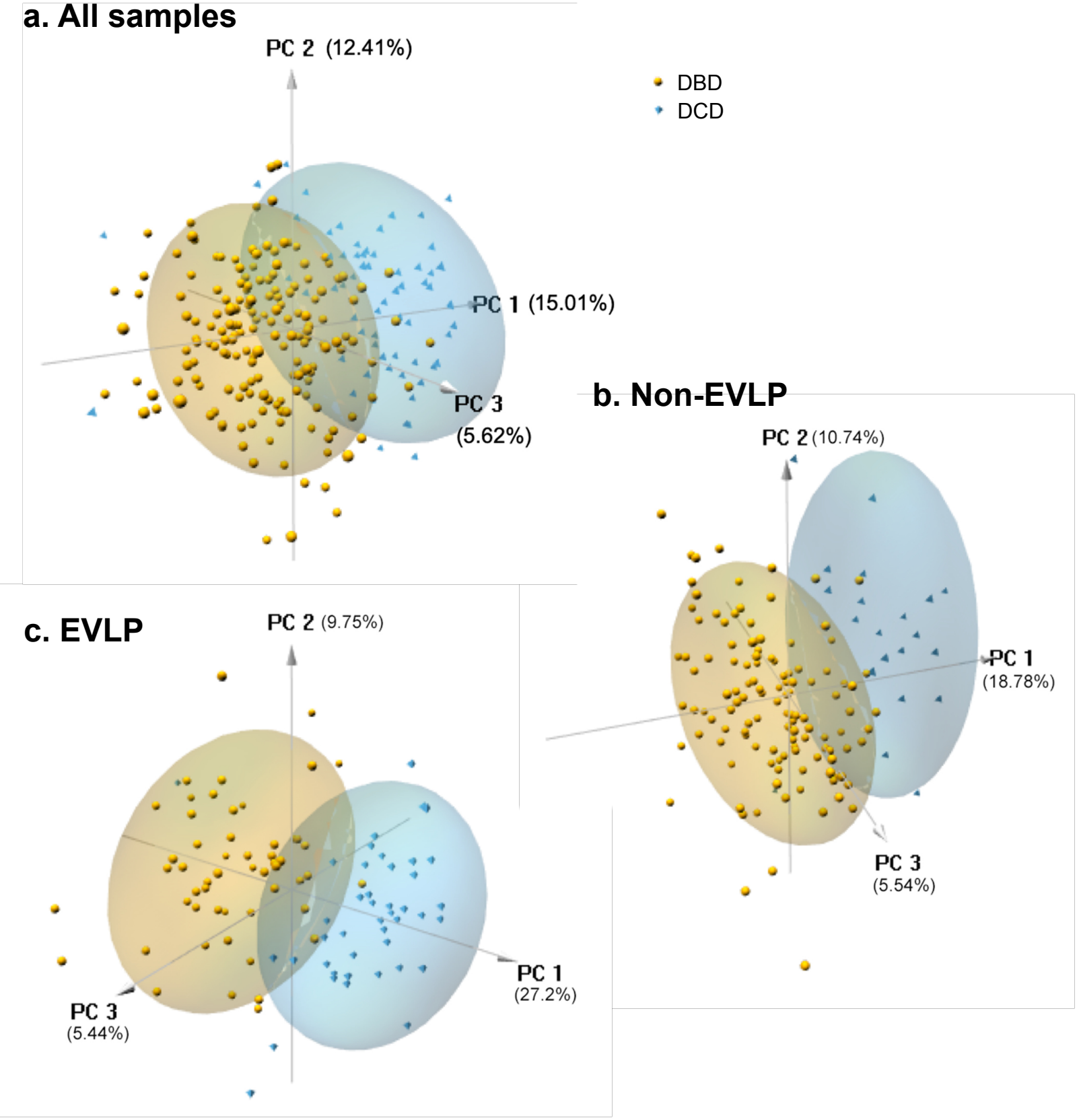

Supplementary Figure 2. Principal Component Analysis: **a.** All samples; **b.** non-EVLP samples only; **c.** EVLP samples only. The numbers in parenthesis show the percent variance explained by the principal component. DBD, donation after brain death; DCD, donation after circulatory death; EVLP, ex-vivo lung perfusion

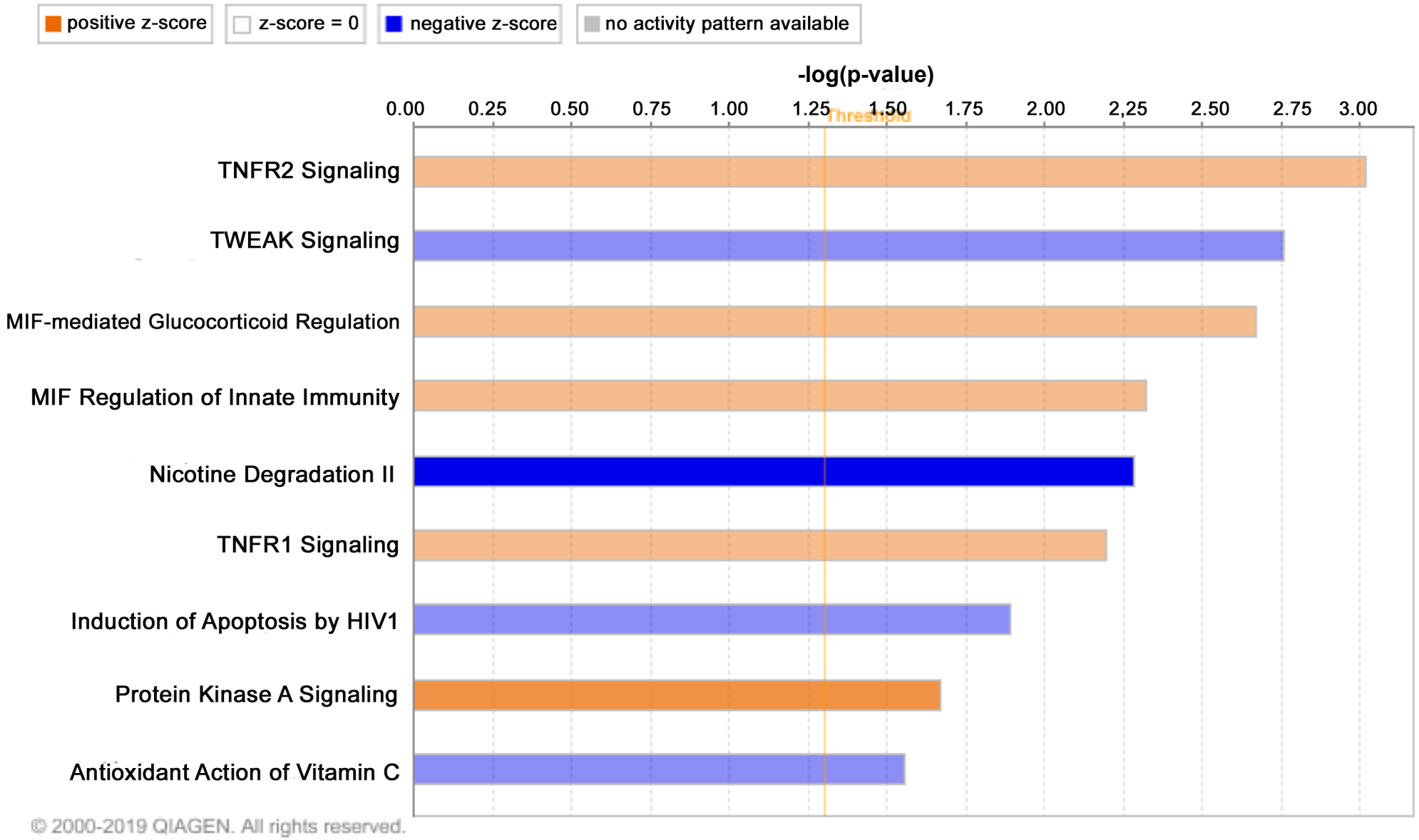

Supplementary Figure 3. Pathways predicted to be activated or inhibited in EVLP vs. non-EVLP, DBD samples
DBD, donation after brain death; EVLP, ex-vivo lung perfusion